REPORT DOCUMENTATION PAGE

Form Approved
OMB No. 0704-0188

Public reporting burden for this collection of information is estimated to average 1 hour per response, including the time for reviewing instructions, searching existing data sources, gathering and maintaining the data needed, and completing and reviewing the collection of information. Send comments regarding this burden estimate or any other aspect of this collection of information, including suggestions for reducing this burden, to Washington Headquarters Services, Directorate for Information Operations and Reports, 1215 Jefferson Davis Highway, Suite 1204, Arlington, VA 22202-4302, and to the Office of Management and Budget, Paperwork Reduction Project (0704-0188), Washington, DC 20503.

1. AGENCY USE ONLY (Leave blank)	2. REPORT DATE	3. REPORT TYPE AND DATES COVERED
	April 3, 1996	Final Report (1994-1996)

4. TITLE AND SUBTITLE
"Microstrain and Defect Analysis of (CL-20) Crystals by Novel X-Ray Methods"

5. FUNDING NUMBERS
N00014-94-0478

6. AUTHOR(S)
Dr. R. Yazici and Dr. D. M. Kalyon

7. PERFORMING ORGANIZATION NAME(S) AND ADDRESS(ES)
Stevens Institute of Technology
Highly Filled Materials Institute
Castle Point on the Hudson
Hoboken, NJ 07030

19960809 166

9. SPONSORING/MONITORING AGENCY NAME(S) AND ADDRESS(ES)
Dr. Richard S. Miller, Code 333
Program Manager
Mechanics & Energy Conversion S&T Division
Office of Naval Research - 800 N. Quincy St.
Arlington, VA 22217

10. SPONSORING/MONITORING AGENCY REPORT NUMBER

11. SUPPLEMENTARY NOTES

12a. DISTRIBUTION/AVAILABILITY STATEMENT
Approved for public release; distribution is unlimited.

12b. DISTRIBUTION CODE

13. ABSTRACT *(Maximum 200 words)*

This project has demonstrated the capabilities of a new x-ray technique to detect and quantify microstrains and defects in semi-crystalline energetic materials. The technique is based on simultaneous rocking-curve analysis of individual particles. The technique was applied to the analysis of CL-20 particles to investigate the effects of synthesis, grinding and static loads on the extent of microstrain and defect development. Overall, these demonstrated capabilities can be employed by DoD in investigating and distinguishing between methods of crystallization and processing by utilizing measures of microstrain and on exploring relationships between crystal defect and microstrain density distributions versus ultimate properties.

14. SUBJECT TERMS			15. NUMBER OF PAGES
			16. PRICE CODE
17. SECURITY CLASSIFICATION OF REPORT	18. SECURITY CLASSIFICATION OF THIS PAGE	19. SECURITY CLASSIFICATION OF ABSTRACT	20. LIMITATION OF ABSTRACT
Unclassified	Unclassified	Unclassified	

FINAL REPORT

BMDO-ONR PROJECT

R & T Project Code #S400040SRS01

"MICROSTRAIN AND DEFECT ANALYSIS OF CL-20 CRYSTALS BY NOVEL X-RAY METHODS"

Submitted to: Dr. Richard S. Miller, Code 333
Program Manager
Mechanics & Energy Conversion S&T Division
Office of Naval Research
800 N. Quincy Street
Arlington, VA 22217

By: Dr. R. Yazici and Dr. D. Kalyon
Highly Filled Materials Institute
Stevens Institute of Technology
Castle Point
Hoboken, NJ 07030

Date: April 3, 1996

19960429 1

DTIC QUALITY INSPECTED 1

TABLE OF CONTENTS

EXECUTIVE SUMMARY

The BMDO-ONR project is focused on the characterization of microstrains and defects in CL-20 crystalline particles. Microstrains and defects are introduced during synthesis and crystal-growth stages of the particles and increase during processing stages such as grinding, mixing and extrusion.

The detection and quantification of these microstrains and defects in a given particle population is a difficult task which requires highly sensitive techniques. In this study, a novel x-ray diffraction technique (XAPS) based on simultaneous rocking-curve analysis of individual particles was successfully applied to CL-20 powders. The effects of synthesis, grinding and static loads on the extent of microstrain and defect development in CL-20 particles were quantitatively determined as frequency versus half-width of rocking curves. The greater half-width values observed for the samples subjected to grinding and static loads indicated greater microstrain and defect density in comparison to as received sample. Thus, our novel x-ray diffraction techniques were successfully demonstrated for the characterization of microstrains.

During this study, new CL-20 crystals were also grown at HFMI with different particle morphologies; and single crystal analyses were carried-out for crystal-structure determination by utilizing Kappa diffractometry. This additional work was carried-out because the crystal structure parameters of CL-20 were required for the dislocation density calculations and there was no information on the CL-20 crystal structure in the literature. Overall, these demonstrated capabilities can be employed by DoD in the investigating and distinguishing between new methods

or procedures of crystallization and processing by utilizing measures of microstrain as a guiding parameter on one hand and on exploring relationships between crystal defect and microstrain density distributions versus ultimate properties on the other hand.

I. INTRODUCTION

CL-20 or hexanitrohexaazaisowurtzitane is a new energetic material which exhibits higher density and heat of formation and is more oxidized than RDX and HMX, the standard energetic nitramines. These superior properties are due to its unique caged structure (isowertzitane) with characteristics of high density, strained ring and high branching, respectively [1, 2}. Superior products have already been demonstrated by replacing the conventional nitramines with CL-20. These include solid rocket propellants, gun propellants and shaped charge explosives.

The combustive properties of energetic materials such as CL-20 depend on their composition and microstructural characteristics such as molecular and crystal structure and particle size distribution [3]. Although, some of these characteristics have been fairly well understood, the effects of more subtle features, such as molecular and crystal defects on the combustive properties of energetics have not been investigated. The presence of micro defects such as misaligned domains and dislocations in single crystallites (particles) are known to increase their chemical activity, by straining the crystal lattice and making more reaction sites available at the domain boundaries and dislocation sites [4-6]. The strain energy of a dislocation is about 8eV for each atom plane threaded by the dislocation while the core energy is in the order of 0.5eV per atom plane [7]. This large positive stain energy means that the free energy of a crystal is increased by the introduction of a dislocation. Processing practices in crystal growth, such as, solution stoichiometry, temperature, catalysts, impurities and even mechanical vibrations could induce defective and partially amorphous structures, that would be invisible to most of the characterization techniques. Highly sensitive and

reliable techniques are required in order to determine quantitatively the extent of these defects in energetics in order to optimize their processing parameters and energetic properties.

The goal of this project was to investigate the applicability of novel x-ray methods to quantitative determination of crystal imperfections, i.e., microstrains and defects in CL-20 particles. For this purpose the most sensitive and novel x-ray diffraction technique (XAPS), developed earlier by Yazici [5, 6, 8-10] and based on the simultaneous rocking-curve analysis of individual particles was applied to CL-20 powders.

II. EXPERIMENTAL PROCEDURES

2.1 Materials

The materials used in this study were two CL-20 powder samples manufactured by Thiokol Corporation and provided by ONR. The two powder samples received had average grain size of 130 microns (coarse) and 6 microns (fine), respectively.

Some of the coarse (130μ) CL-20 powder samples were subject to deformation under static loads to simulate processing conditions. The static loads applied ranged from 600 psi to 2000 psi, and held for 10 minute durations. The deformation experiments were carried-out at two temperatures: 25° and 90°C.

In addition to the as-received powders, new CL-20 crystals were also grown at Stevens with different particle morphologies. These new crystals were grown and used, together with the as-received powders, for crystal structure analysis.

All CL-20 samples were kept in sealed cups with neutralizing water suspension, except during testing. The sealed cups were placed in steel bomb enclosures during storage.

2.2 Characterization Methods

2.2.1 X-Ray Analyzer for Particles (XAPS)

In this study a novel x-ray method X-Ray Analyzer for Particles (XAPS) developed by Yazici, and based on simultaneous rocking-curve analysis of individual particles, was employed to quantitatively determine the microstrain and defect distribution in CL-20 energetic crystals. XAPS is the most sensitive method for measuring the degree of imperfection and lattice misalignment of individual crystallite through x-ray rocking-curve half-width measurements. (See Figures 1 and 2).

Briefly, in XAPS rocking-curve technique the powder sample is irradiated with a crystal monochromatized parallel x-ray beam. Each reflecting crystalline particle acts independently as the second crystal or test crystal of a double-crystal-diffractometer. Those particles which are in reflecting positions give rise to individual diffraction spots along the Debye arc. (Fig. 1). Each diffracting spot emanating from the powder sample is registered as a function of location and intensity by a linear position-sensitive detector (PSD) which is aligned parallel to the Debye arc. After a short exposure the x-ray intensity spectra are collected by a multichannel analyzer (MCA) and stored by a computer. When the data transmission is completed, the sample is rotated automatically by a chosen increment (1 minute of arc) before the next exposure is started. This step-wise rocking process is repeated until the entire angular range of the grain reflections

are recorded (20 minutes of arc). The rocking-curve for each particle as well as for the entire particle population is computed by analyzing the entire reflection matrix. The rocking-curve half-width (full width at half maximum intensity) provides a measure of microstrain and angular lattice misalignment induced by dislocations within the diffracting grain. (Fig. 2).

The width at half the maximum intensity of the rocking-curve (half-width) or (β) provides a measure of the angular lattice misalignment of the crystallite. Thus, the half-width (β) values provide information about the local densities of the accumulated excess dislocations of one sign i.e., or same orientation with respect to lattice directions.

Some relationships between the distribution of excess dislocations and the resultant rocking-curve profiles are schematically shown in Fig. 2. If the profile is smooth, a homogeneous distribution of excess dislocations would, as marked in "deformed" exist. If, on the other hand, a multipeaked profile is produced, the excess dislocations are heterogeneously distributed, giving rise to distinct lattice tilts as would be encountered, for example, in grains with subgrain boundaries, as marked "polygonized". The angle between the subpeaks of such rocking-curves would then represent the relative misorientation of adjacent lattice domains or subgrains, whereas the width of well resolved subpeaks indicate the degree of internal distortion in these domains. Annealed grains with low excess dislocation densities give rise to smooth rocking-curves with small β values as marked in "annealed".

Assuming that the excess dislocations are randomly located in the grains and thus can be represented by a Gaussian distribution, the excess dislocation

density is determined by $D = \beta^2/9b^2$, where b is the magnitude of the Burgers vector. If the excess dislocations are aligned in the subgrain boundary and the tilt angle of adjacent subgrains, ε, is measured, the excess dislocation density in the subgrain boundary $D_{SB} = \varepsilon/3bt$, where t is the subgrain size (11). If resolvable, the subgrain size can be measured from the images of X-ray reflection topographs.

The microstrains, i.e., the residual strains (and stresses) in individual crystallites or particles, induced by the excess dislocations can also be calculated from the excess dislocation density D values, provided that the exact nature and distribution of the excess dislocations are known and the crystal structure and physical constants are given. The micro-stresses associated with a dislocation is biaxial in nature and vary inversely with distance from the dislocation core. Although the stresses at the core reach to infinite values, more reasonable stresses are induced over the average body of the crystal (7).

A Picker 4-circle goniometer was utilized for XAPS experiments. CuK_α radiation monochromatized with a Si (111) crystal at 35 kV and 20 mA was used. Five to fifteen minute timed exposures were applied at each rocking step. Three-hundred to one-thousand individual particles were evaluated from each sample.

2.2.2 Other Methods

Wide-Angle X-ray Diffractometry (WA-XRD) was utilized for determination of the degree of crystallinity of the CL-20 powders. Computer aided deconvolution methods with Images software were applied to determine the relative contributions of the amorphous and crystalline portions of the samples from their

diffraction patterns. The unit used was Rigaku DXR-3000 diffractometer system. CuK_α radiation at 40 kV and 20 mA, and a graphite monochromation with focusing geometry were used for all WA-XRD runs.

Kappa diffractometry was used to carry-out single crystal analysis and to determine the crystal structure parameters. This work was carried-out because the crystal structure parameters were required for dislocation density calculations; and because there was no information on the CL-20 crystal structure in the literature. A Nonius Difractis 586 x-ray unit and CAD4 and NRC software packages were used for single crystal analysis.

Scanning electron microscopy (SEM) was used to examine the particle morphology. A JEOL 840 SEM with EDX was utilized for this purpose.

Fourier transform infrared spectroscopy (FTIR) and differential scanning calorimetry (DSC) were also applied to evaluate the molecular polyform and the transition temperatures, respectively, of the CL-20 powders.

III. **RESULTS**

Typical XAPS rocking-curve data, i.e., intensity vs. position vs. rotation, as stored in the computer memory is shown in Fig. 3. The data shown is only a small portion of a single rocking-curve run where 2/3 of the rotations and 2/3 of the channels were omitted for simplification. The analysis program locates the intensity from a specific particle at a specific MCA channel(s) at a specific rotation step and follows its variation at the same channel(s) in each rotation and obtains the rocking-curve distributing profile before calculating the width at half

maximum. This procedure is carried-out for each reflecting grain. Twenty to one-hundred grains are analyzed in each run.

3.1 Coarse Versus Fine (Ground) CL-20 Powders

The results of the XAPS rocking-curve analysis of the as-received coarse and fine CL-20 powder samples are shown in Figs. 4 and 5, respectively. In these figures, the statistical distribution of the half-width values of the individual particles are exhibited as the particle frequency observed for each half-width value. In these graphs, the larger half-width values emanate from those particles which constitute high microstrains and defects, and, conversely the smaller half-width values emanate from those particles which constitute less defects and low microstrains. The rocking-curve half-width mean values of the fine powder (5.1 minutes of arc) was measurably larger than that of the coarse powder (4.2 minutes). Also, the maximum half-width value observed in the fine powder (38 minutes) was considerably higher than the coarse powder (18 minutes).

Assuming that the excess dislocations are randomly located in the grains, the excess dislocation density $D = \beta^2/9b^2$ can be calculated for each case. Taking the Burgers vector b = 8.84 Ångstrom, then the excess dislocation density values can be determined. For the as-received coarse powder the excess dislocation density is 2.1 $10^7/cm^2$, and for the as-received fine (ground) powder it is 3.1 $10^7/cm^2$.

Fine CL-20 batch was obtained by grinding of the as-grown particles. The higher half-width values of the fine CL-20 powder is, therefore, a direct measure of the effect of the grinding process on the crystal defects. Thus, the grinding process

applied has increased the lattice imperfections and defects in the CL-20 particles. The XAPS rocking-curve technique can, therefore, be utilized to quantitatively determine the effects of grinding on crystal defects.

Typical SEM images of the coarse and fine CL-20 particles are shown in Figs. 6a, b, and c, respectively. Some qualitative evidence of defects induced during crystal growth and grinding are indeed visible on these microphotographs.

The typical results of the WA-XRD scans are shown in Figs. 7 and 8 for the coarse and fine powders, respectively. According to the deconvolution analysis carried-out on these patterns the degree of crystallinity of the CL-20 powders was in the range of 90% to 93%. The difference in the degree of crystallinity of the coarse and fine powders was negligible.

The FTIR analysis of the powders was carried-out (see Fig. 9) and the purity of the ε polymorph was established using the methods proposed by an earlier publication [ref. 2]. The presence of the doublet between 8.20 cm^{-1} and 850 cm^{-1} (and the lack of a single peak) establishes the purity of the ε polymorph. ε-CL-20 is the most stable and energetically favorable polymorph.

The DSC scan of CL-20 powder is shown in Fig. 10. According to this DSC scan the CL-20 crystals exhibit an exothermic transition (melting) at 168° C. The heat release is 3.46 cal/g.

3.2 CL-20 Powders Subjected to Deformation

As noted earlier specimens of the coarse CL-20 powder were compressed using a modified compression molding machine. When the coarse CL-20 particles were loaded at 25°C they were fractured in a brittle fashion (see Fig. 11). Because of the brittle behavior of the CL-20 at room temperature (no dislocation activity), the microstrain and the defect density of the particles were not affected. Only the particle size was reduced.

The results of the XAPS rocking-curve analysis of the coarse CL-20 powder subjected to deformation under static loads at 90°C are shown in Figs. 12 and 13. The powder in Figure 12 was subject to 2,000 psi static load for 10 minutes duration at 90°C. As shown in Fig. 12, the mean half-width value of the coarse CL-20 particles increased to 9.4 minutes-of-arc from the 4.2 minutes-of-arc of the as-received particles. The statistical distribution of the half-width values, as measured with frequency, was substantially broadened and the maximum half-width value reached to 40 minutes-of-arc. The mean excess dislocation density for this sample is 1.1×10^8 /cm^2, and the maximum is 1.9×10^9 /cm^2.

The powder in Fig. 13 was subject to 600 psi static load for 10 minutes time at 90°C. As shown in Fig. 13, the mean value of the half-width for these particles reached to 5.3 minutes of arc. The mean excess dislocation density for these particles is 3.4×10^7/cm^2, and the maximum is 3.9×10^8/cm^2.

In this work, the CL-20 particles were subject to static loads at 90°C in order to emulate the uniaxial compression involved in the thermo-mechanical conditions that they would experience during processing such as mixing and extrusion.

During these processes high shear stresses are also generated and the particles, together with the binder, all go through shear deformations. Invariably, it is the excess shear stresses that cause the microplastic deformations in the crystals. Under shear stresses, crystals tend to generate dislocations along their slip-planes and shear deform by slip. The "characteristic slip-plane" of a crystal tends to be the lattice plane where the separation between the atoms/molecules is maximum.

By applying normal loads to randomly oriented crystallite particles, "resolved shear stresses" are generated along the "characteristic slip-plane" of each particle. The magnitude of the shear stress would vary depending on the orientation angle of the characteristic slip-plane and the characteristic slip direction of the given particle with respect to the direction of the applied normal stress. For the angle between the applied normal stress direction and the characteristic slip plane normal being ϕ, and the angle between the slip direction and the slip-plane normal being λ, the relationship between the applied normal stress $\sigma_{app.}$ and the resolved shear stress τ_{rss} (on the characteristic slip system of a single crystal) is given by [7]:

$$\tau_{rss} = \sigma_{app.} \cos \phi \cos \lambda.$$

This shear stress resolved on the characteristic slip-plane and in the slip direction of single crystal ranges from zero, for either $\phi = 0$ or $\lambda = 0$, to maximum, for $\phi = \lambda = 45^{o}$. The maximum resolved shear stress is

$$\tau_{rss\,(max.)} = 1/2\ \sigma_{app.}$$

Therefore, in the static-load experiments carried-out in this work, the effective or resolved shear stresses (τ_{rss}) on individual particle slip systems ranged from 0 psi to 1,000 psi for the σ_{app} = 2,000 psi experiment, and 0 psi to 300 psi for the $\sigma_{app.}$ = 600 psi experiment.

During processing i.e., mixing and extrusion, the crystalline particles are mobile and are subject to shear stress under dynamic conditions. In the duration of processing the particles are constantly reoriented and most of them experience the maximum shear stresses generated by the processor as resolved on their characteristic slip system. Therefore, the shear deformations during processing are expected to be more extensive and more uniform among the particle population.

In summary, in these applied static load or simulated processing experiments it was demonstrated that the defects induced by external stresses in the CL-20 particles can be quantitatively determined by the novel XAPS technique. It was shown that, although the defect density of the as received particles is high, the application of external loads increase the excess dislocation density substantially.

3.3 Crystal Structure Analysis

The CL-20 crystal structure information was necessary in order to calculate the dislocation density values from the rocking-curve halfwidth measurements. Since there was no crystal structure information on CL-20 available in the literature, the analysis of the crystal structure was undertaken at HFMI. Crystal structure analysis was first carried-out on the as-received coarse CL-20 particles. However, because of the relatively high imperfections in these particles the

measurements exhibited significant scatter precluding precision in the lattice parameter calculations. In order to be able to characterize the crystal structure of CL-20 accurately, CL-20 crystals were grown from solution at HFMI. For this purpose the as-received CL-20 particles were dissolved in various solvents and CL-20 was re-crystallized from solution. Different particle morphologies were obtained with different solvation experiments (see Fig. 14 a-d).

The crystal structure of ε-CL-20 was determined using one of the crystals grown at HFMI. The results of these preliminary studies indicated the following:

CL-20

crystal system:	Monoclinic
unit cell parameters:	a = 8.84 (2) Å
	b = 12.50 (4) Å
	c = 13.36 (2) Å
	$\alpha = \gamma = 90^{o}$
	$\beta = 106.8^{o}$ (1)
unit cell volume:	V = 1,414.3 $Å^3$

number of molecules per unit cell: z = 4

x-ray density: d = 2.04 g/cc

$$\left(d \frac{zM_W}{V N_A} \right) \text{(molecular wt. = 438.24)}$$

IV. CONCLUSIONS

The applicability of the novel x-ray method XAPS to the quantitative determination of crystal defects and excess dislocation density of the CL-20 crystals were successfully demonstrated.

It was shown that the defect structure of CL-20 is affected by processing conditions such as grinding and high temperature deformation. The high sensitivity of the XAPS rocking-curve technique was essential in detecting minute increases in defect structure especially under very low loads.

It was shown that the as-received CL-20 crystals contain about seven to ten percent amorphous regions. The possibilities in growing CL-20 crystals with higher crystallinity and different particle morphologies were demonstrated. The CL-20 crystal-structure was also determined.

V. FUTURE WORK

This investigation has demonstrated that XAPS is a novel enabling technology to characterize the microstrain and defect density distributions in energetic crystallites. This demonstrated technology can be used further to elucidate the following:

1) systematic study of the effects of processing variables on the defect structure of CL-20 crystals

2) correlation of defect structure to performance of the CL-20 crystals

3) correlation of defect structure to crystal growth parameters

4) comparative evaluation of CL-20 crystals manufactured by different methods and procedures.

REFERENCES

1. "CL-20 Promising New Energetic Material, an internal publication of Thiokol Corporation, Marshall, Texas (1995).

2. R. L. Willer, D. J. Park and P. J. Kaste, "Development of CL-20 TPE LOVA Gun Propellants", an internal publication of U.S. Army Research Laboratory, Aberdeen Proving Ground, MD (1995).

3. "Chemistry and Technology of Explosives", Vol. 4, T. Urbanski, Pergamon Press, New York (1990).

4. "X-ray Analysis of Accrued Damage in Stress Corrosion and Corrison-Fatigue", S. Weissmann, R. Yazici, T. Takemoto, T. Tsakalakos and I.R. Kramer, ONR R-2 Interim Technical Report, 1979, (a copy is attached).

5. "Determination of Prefracture Damage in Fatigued and Stress Corroded Materials by X-ray Double-Crystal Diffractometry", R. N. Pangborn, R. Yazici, T. Tsakalakos, S. Weismann and I.R. Kramer, NBS Special Publication 567, p. 433 (1979).

6. "Defect Structure Analysis of Polycrystalline Materials by Computer-Controlled Double Crystal Diffractometer with Position Sensitive Detector", R. Yazici, W. Mayo, T. Takemoto and S. Weissmann, J. Appl. Crystallography, 16 89 (1985).

7. G.E. Dieter, "Mechanical Metallurgy", p. 124, McGraw Hill, New York, (1986).

8. X-Ray Measurements of Long-Range Strains: A Bridge Between Micromechanics and Macromechanics", S. Weissman, Z. H. Kalman, J. Chaudhuri, R. Yazici and W. Mayo, In Residual Stress and Stress Relaxation, ed. Eriic Kula and Volker Weiss, Plenum Pub. (1982).

9. "Determination of Thermally and Mechanically Induced Internal Stresses in MMC by X-Ray Methods", R. Yazici, K. E. Bagnoli and Y. Bae, in Nondestructive Monitoring of Materials Properties, eds. F. Holbrook and J. Bussiere, MRS publications, vol. 142 (1988).

10. "Determination of Texture and Internal Strains in Metal-Matrix Composites by X-rays", R. Yazici, S. Han and D. Gultekin, in Application of Neutron and X-ray Scattering to Materials Problems, TMS Fall Meeting (1990).

11. P. B. Hirsch, Progress in Metal Physics 6, p. 282-283 Pergamon Press, New York (1956).

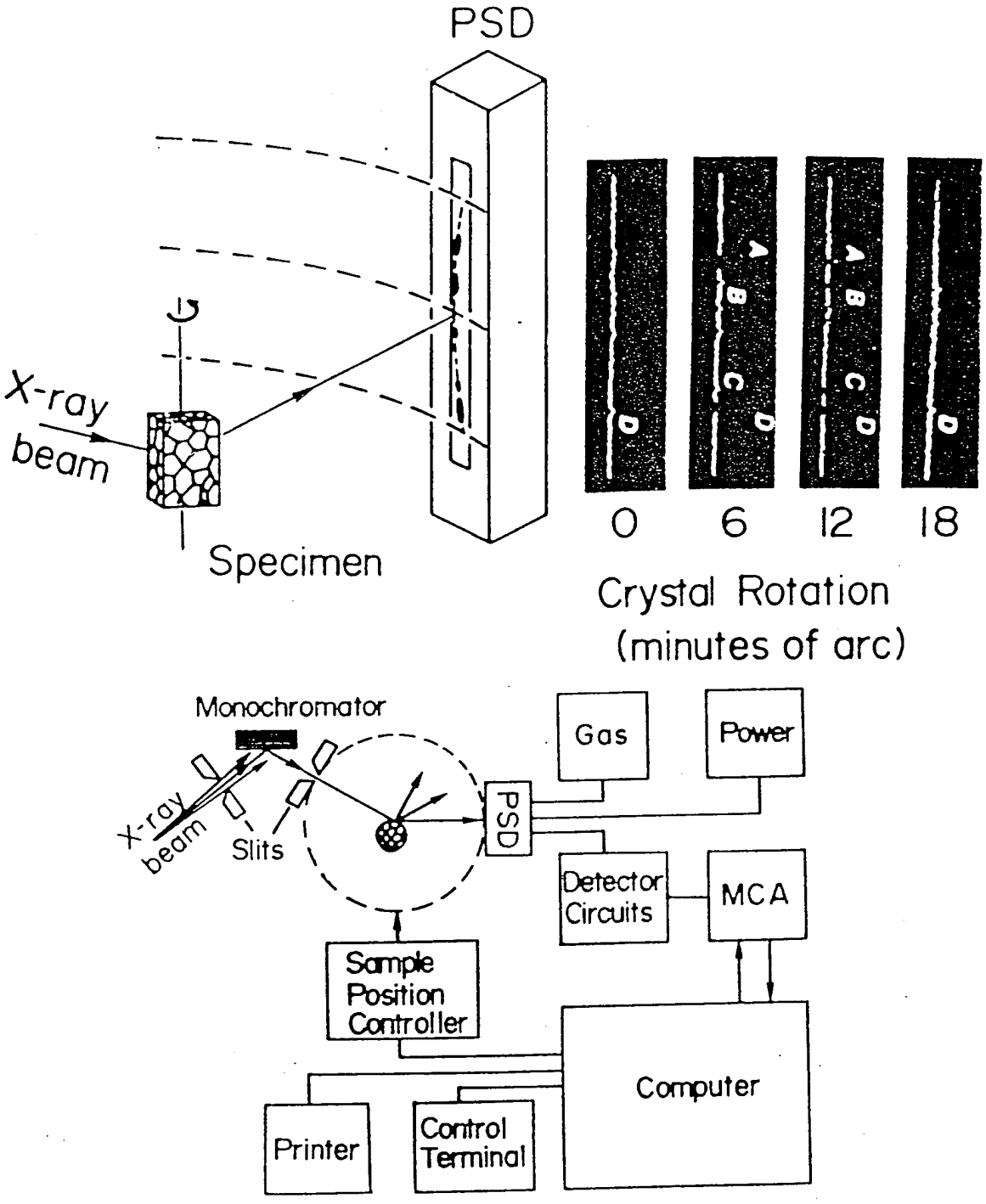

Fig. 1. Principle of operation of XAPS particle rocking curve analyzer.

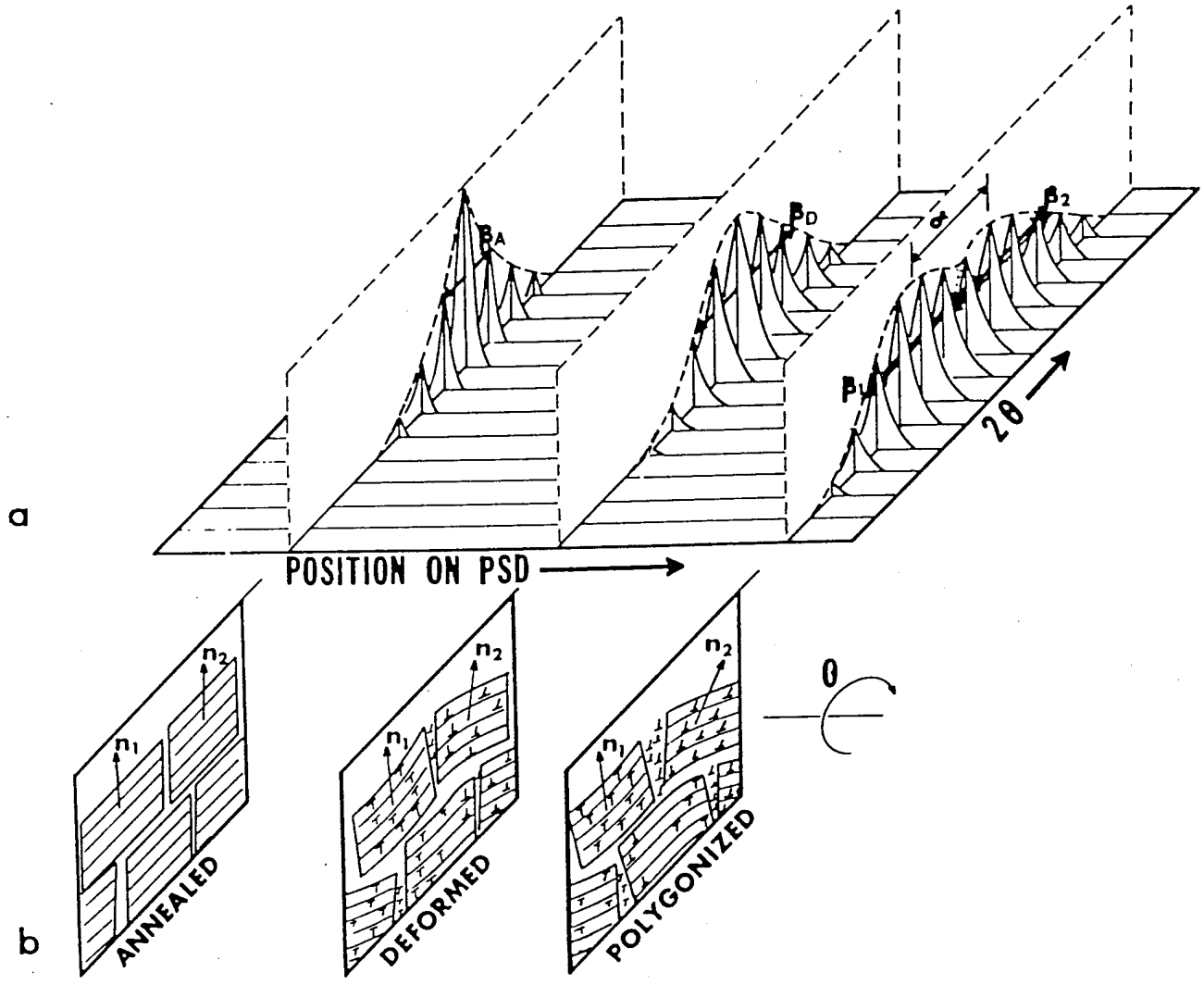

Fig. 2. Rocking curve and particle defect structure characteristics (schematic): a) construction of rocking curves, b) state of the related particle defect structures

Fig. 3. XAPS Rocking-Curve Step Scan Patterns

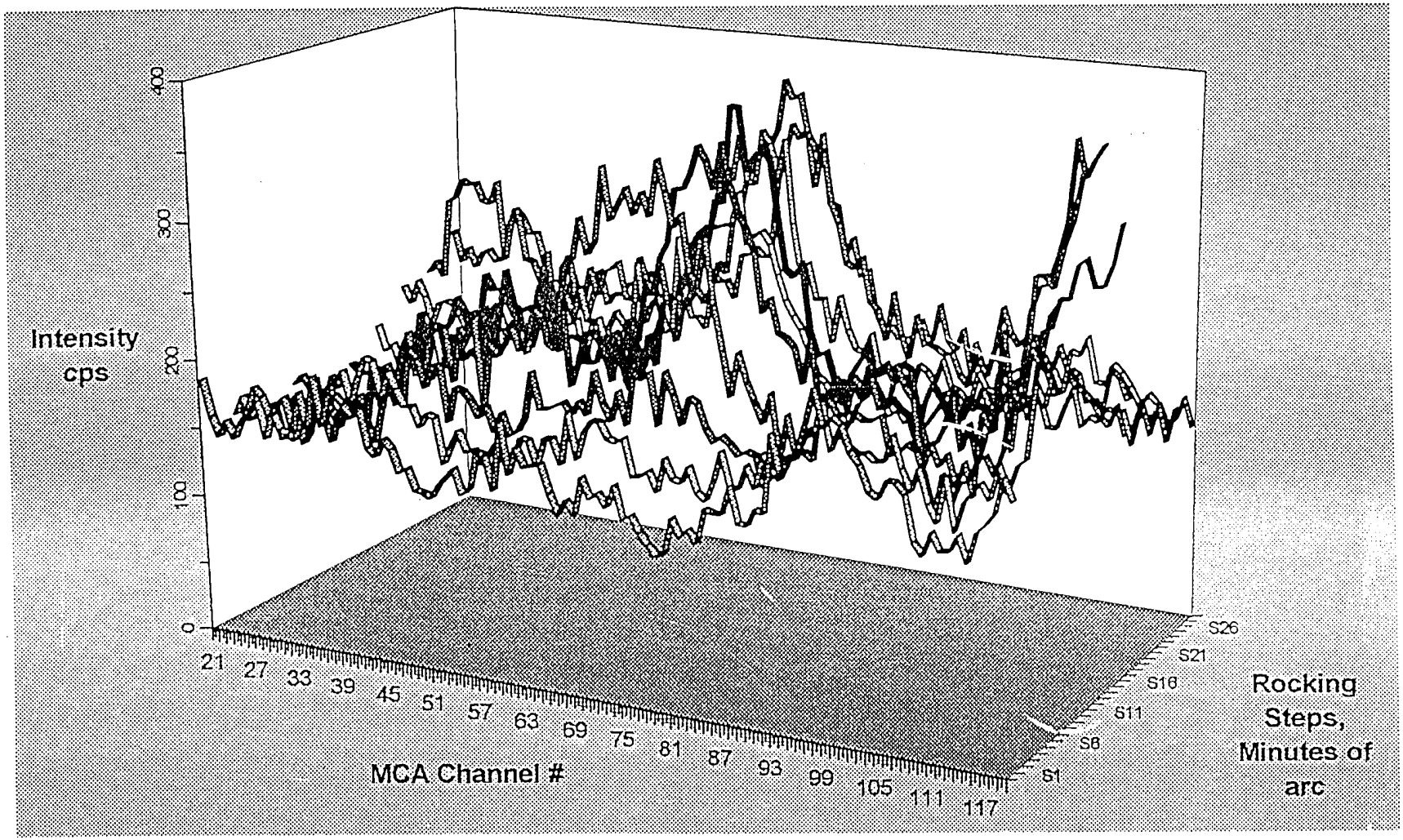

Fig. 4. As-Received Coarse CL-20 Particle-Defect Half-Width Distribution by XAPS

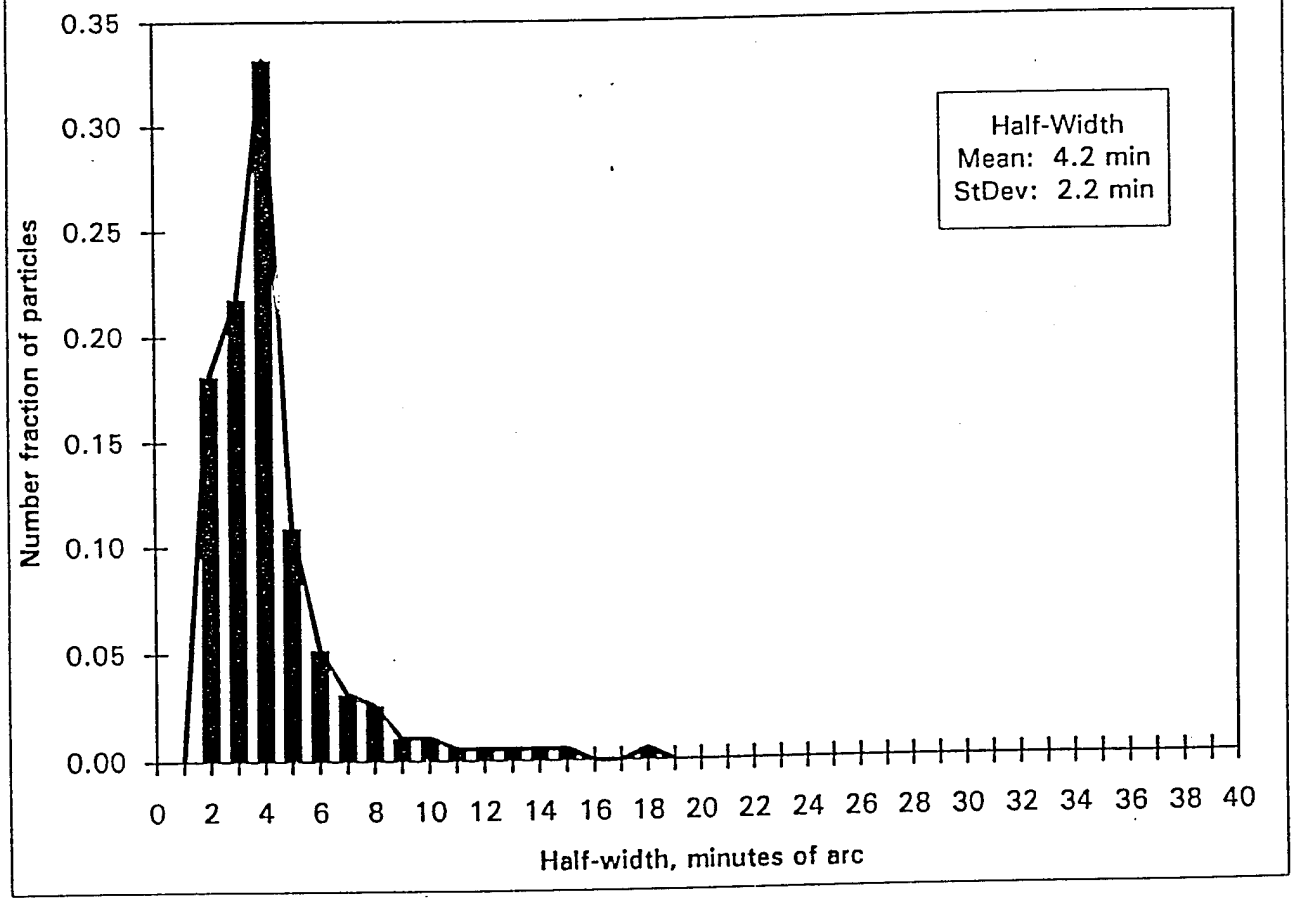

Fig. 5. As-Received Fine CL-20 Particle-Defect Half-Width Distribution by XAPS

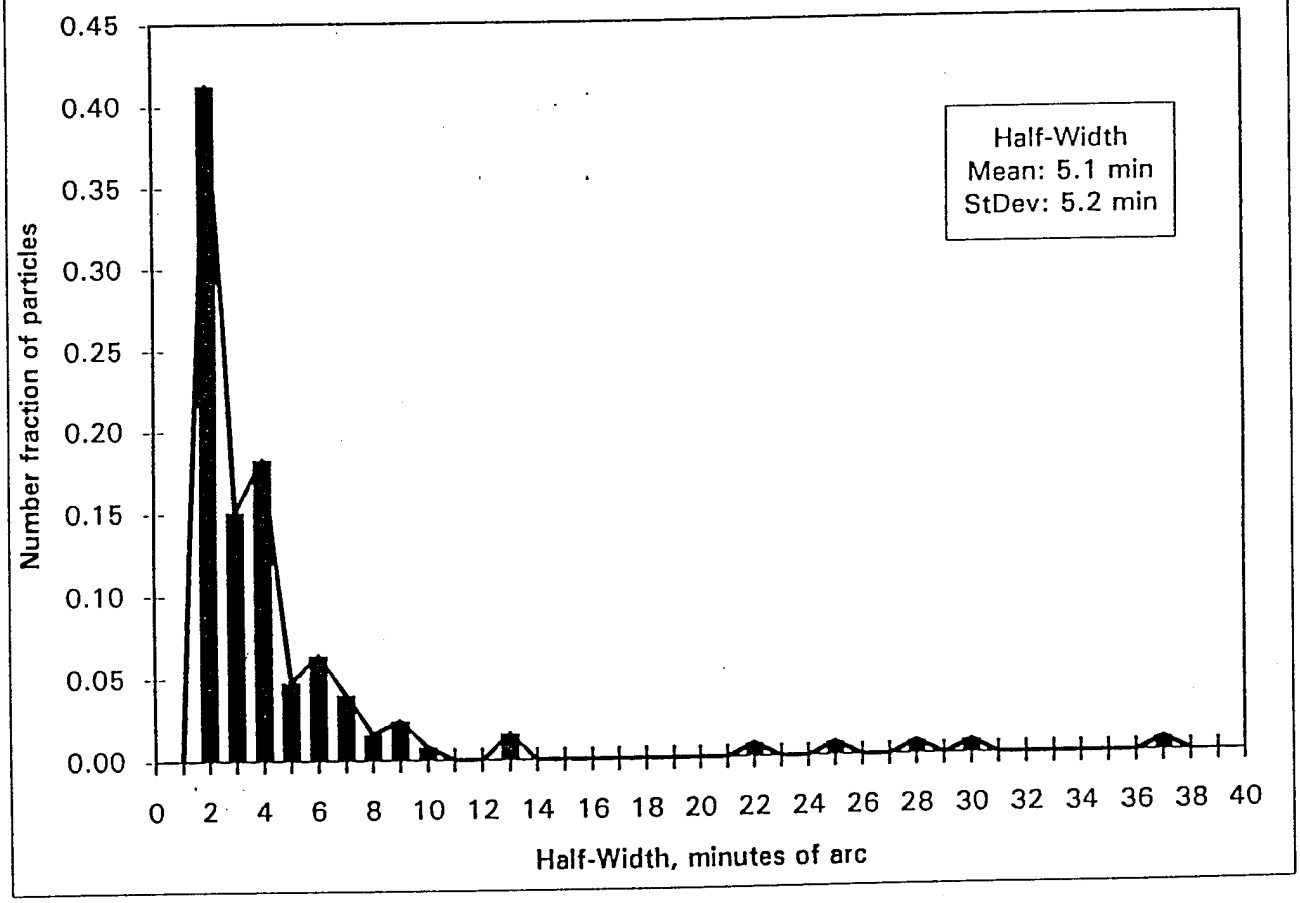

a)

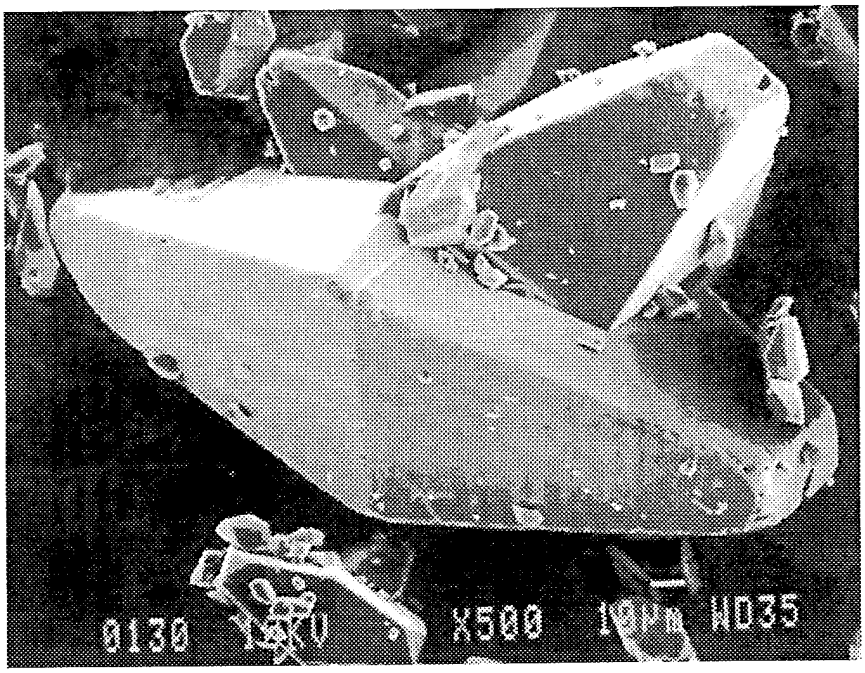

b)

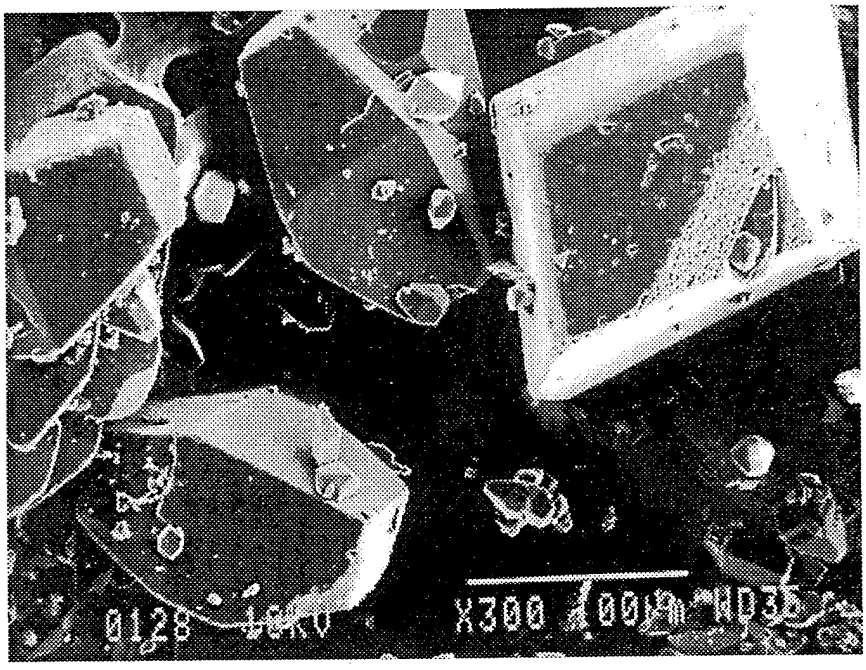

Fig. 6. As received CL-20 particles: coarse powder (a) x500, (b) x300; fine powder (c) x2000.

c)

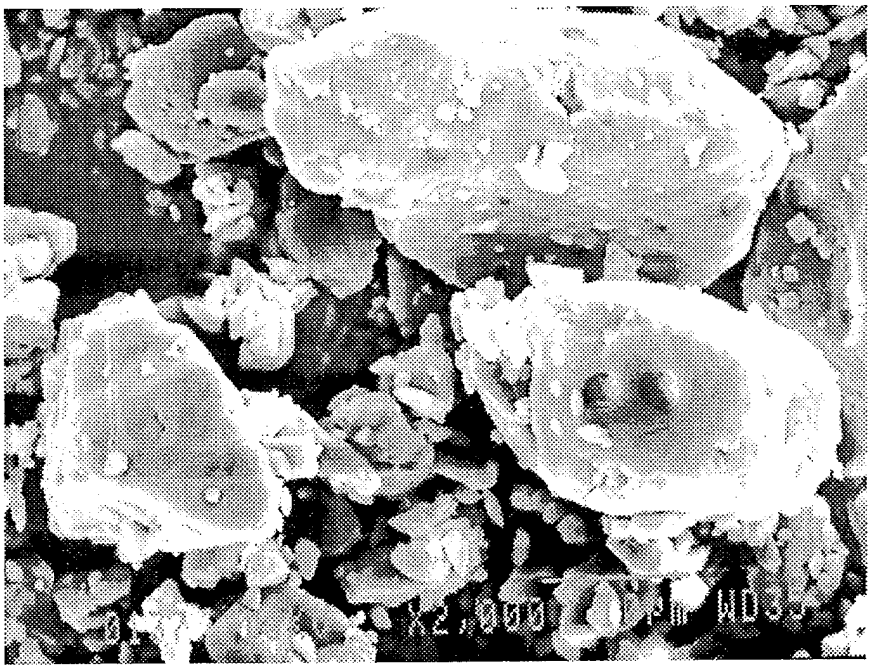

Fig. 6. As received CL-20 particles: coarse powder (a) x500, (b) x300; fine powder (c) x2000.

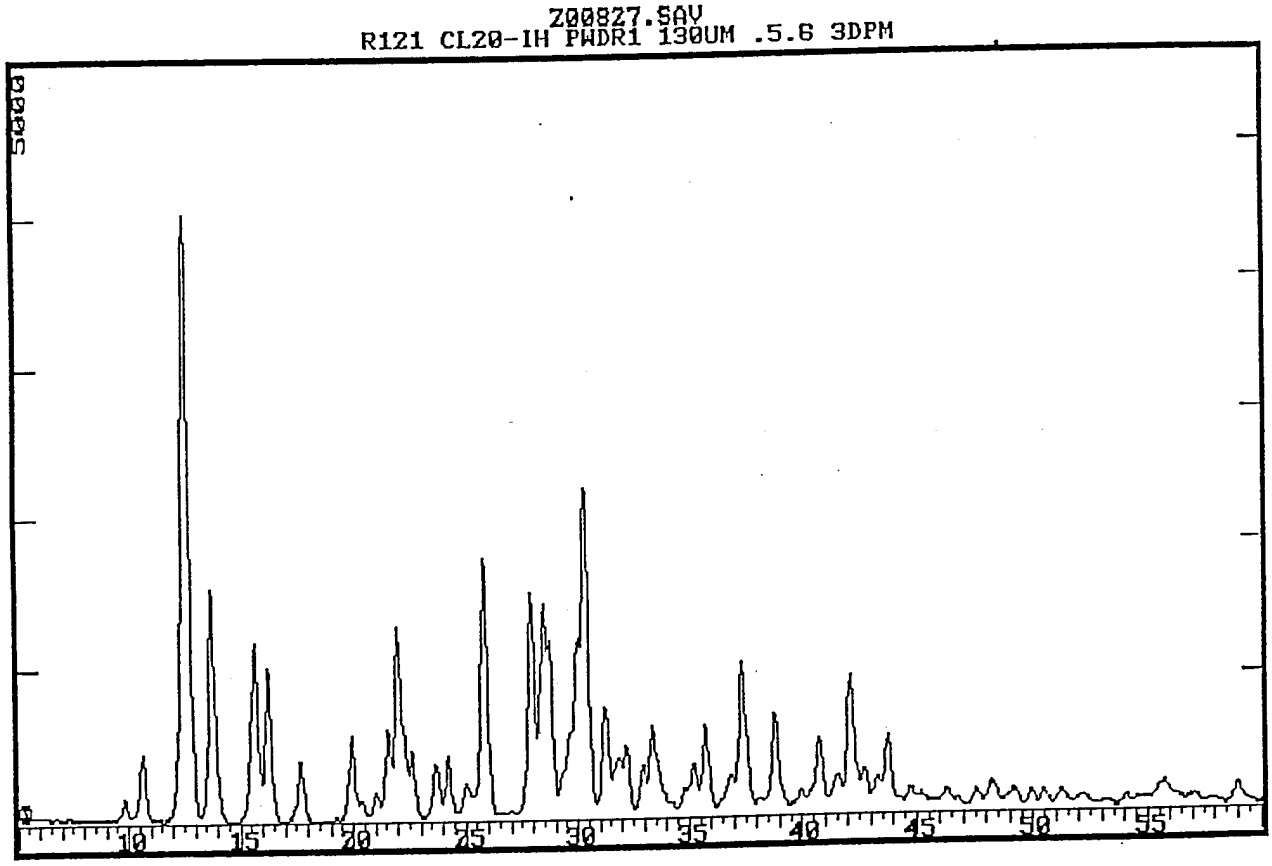

Fig. 7. WA-XRD pattern of coarse CL-20 powder

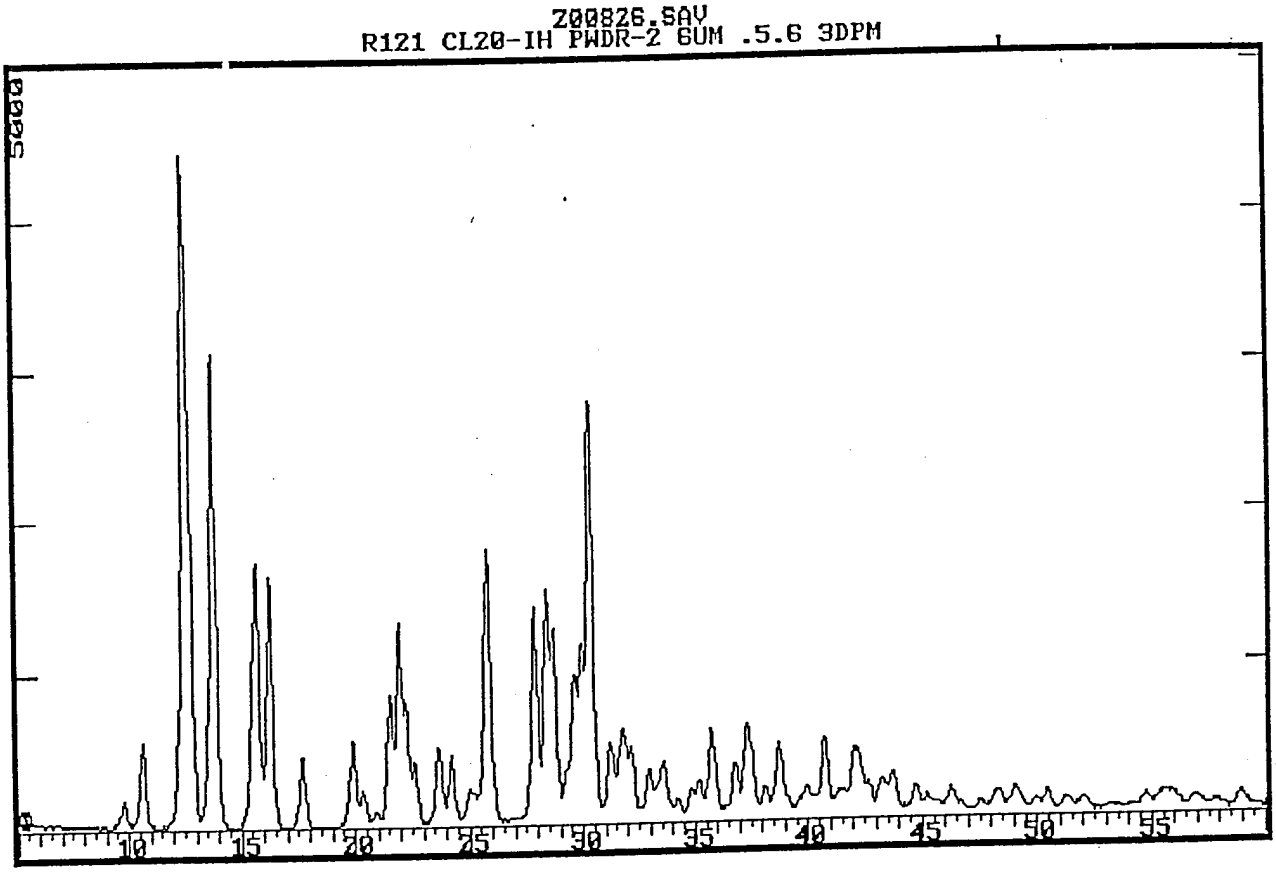

Fig. 8. WA-XRD pattern of fine CL-20 powder

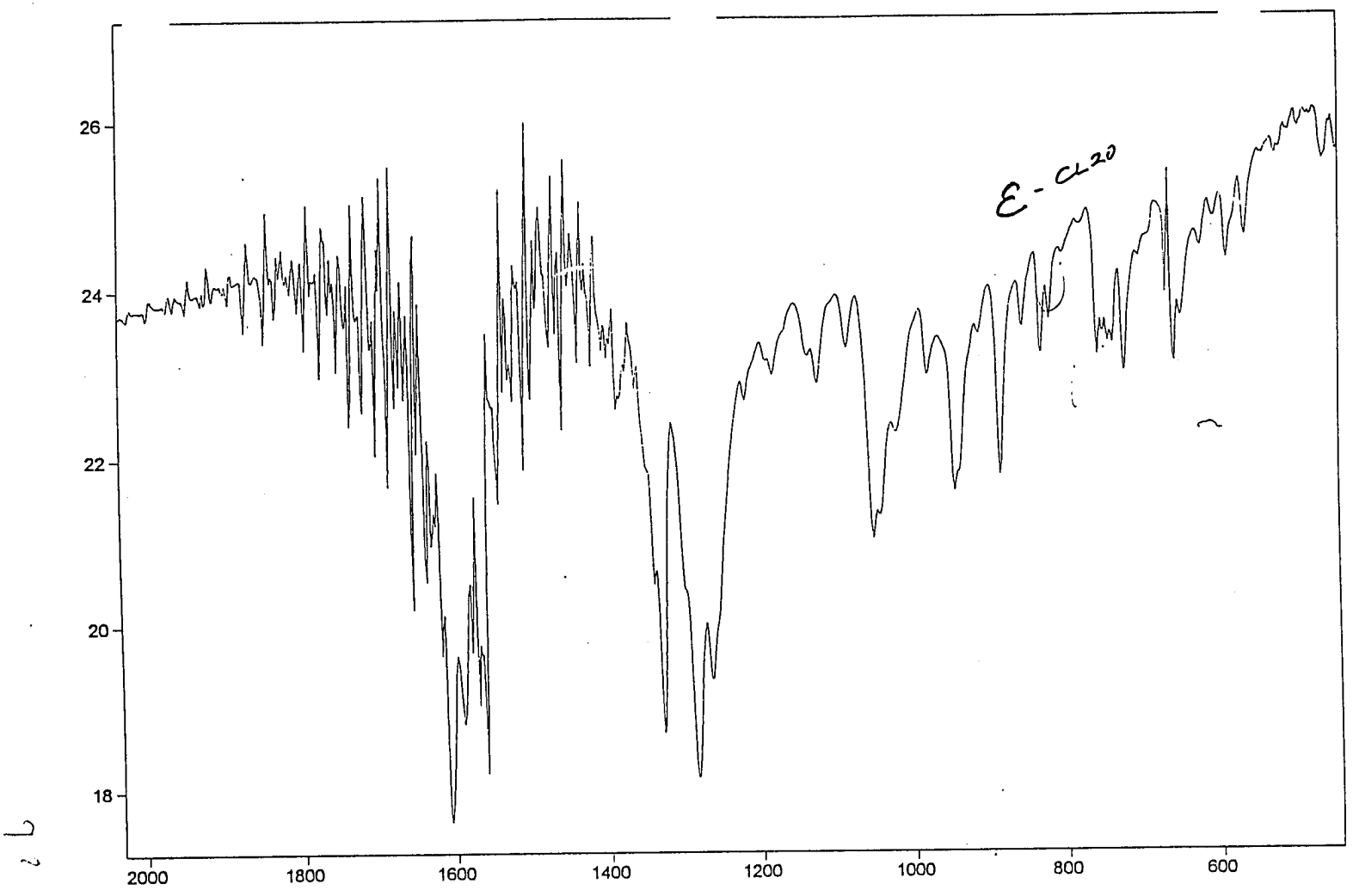

Transmittance / Wavenumber (cm-1)

File # 2 = YAZICI

CL20 , 120u

Number of Scans= 32 Apodization=

1/18/96 1:54 PM Res=4 cm-1

Fig. 9. FTIR spectrum of the CL-20 powders

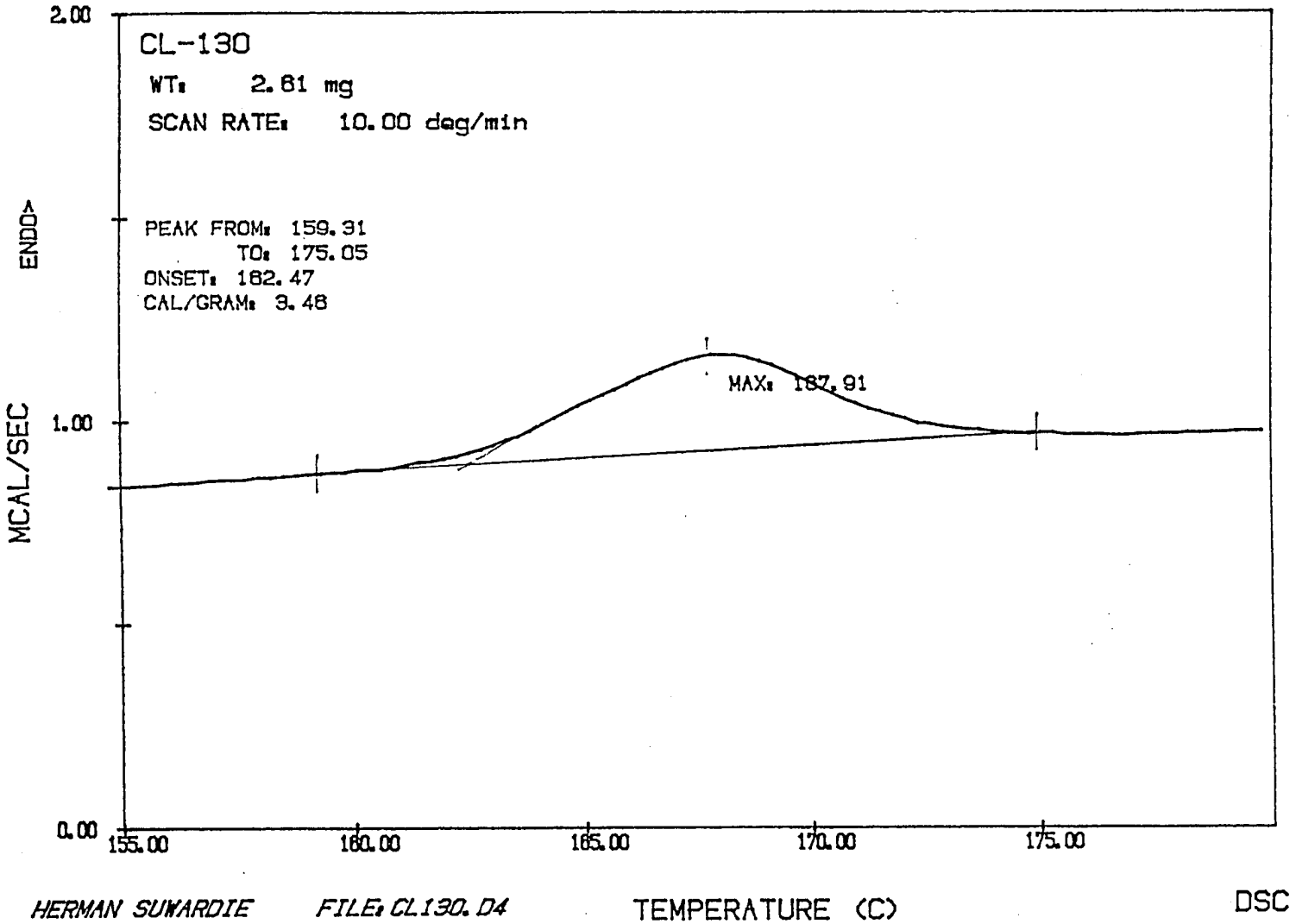

Fig. 10. DSC graph of CL-20 powders

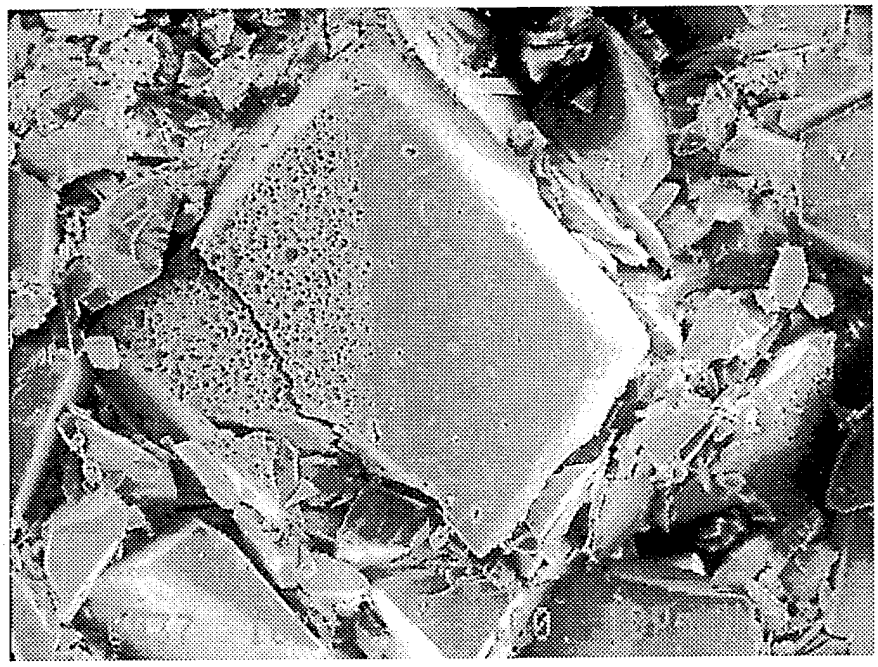

Fig. 11. Coarse CL-20 particles fractured under static load at 25°C.

Fig. 12. **Deformed Coarse CL-20 Particle-Defect Half-Width Distribution by XAPS**

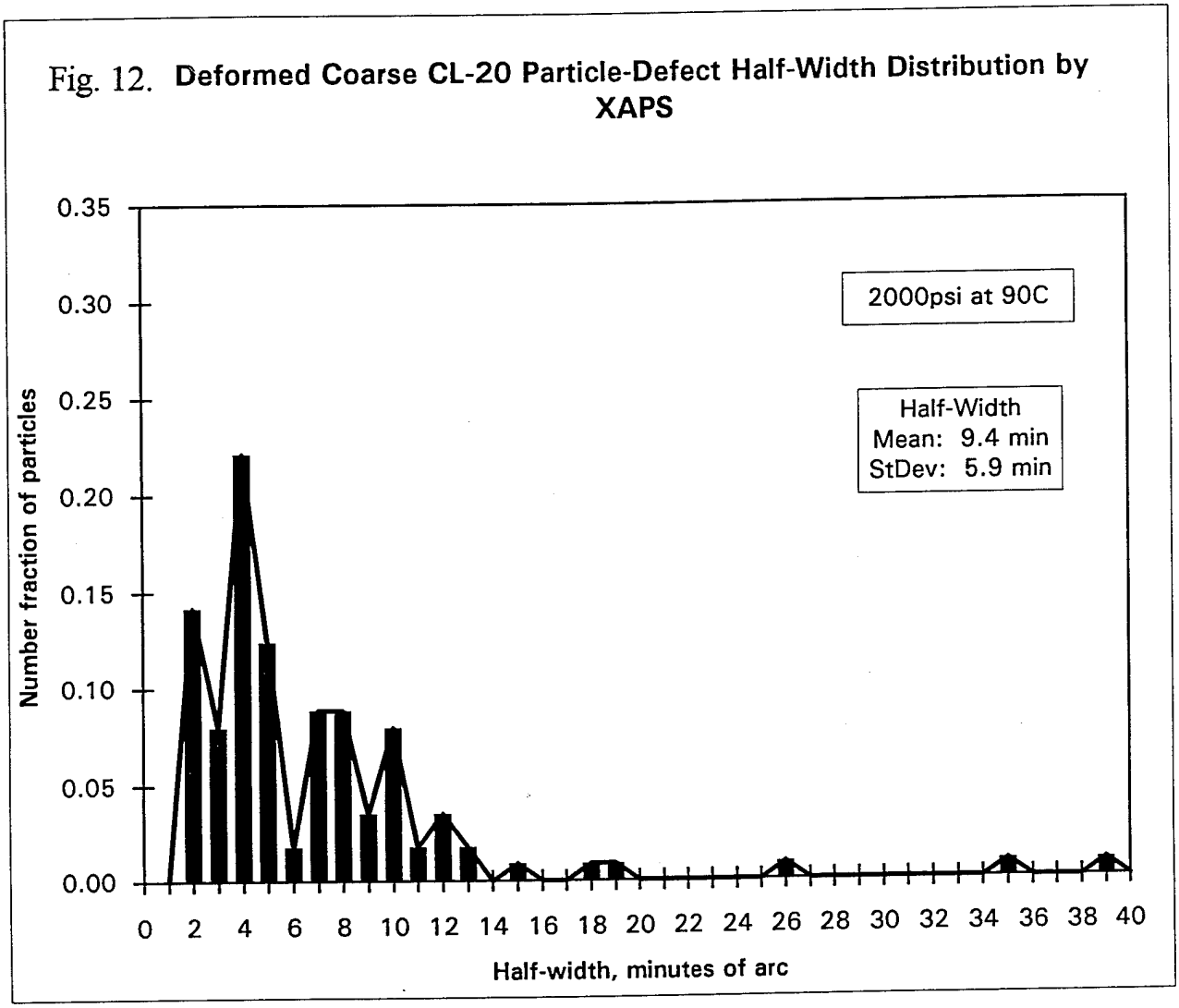

Fig. 13. **Deformed Coarse CL-20 Particle-Defect Half-Width Distribution by XAPS**

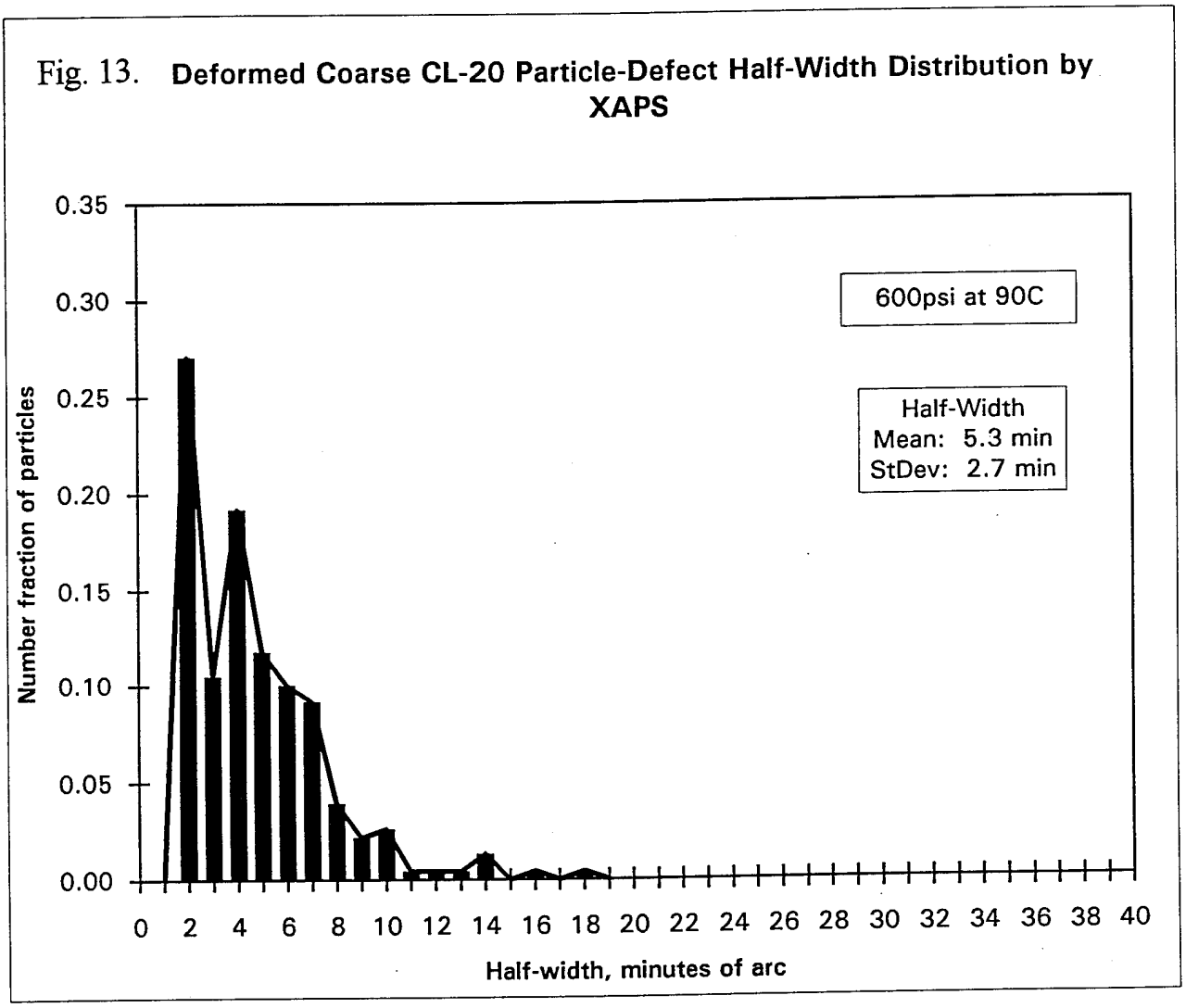

a)

b)

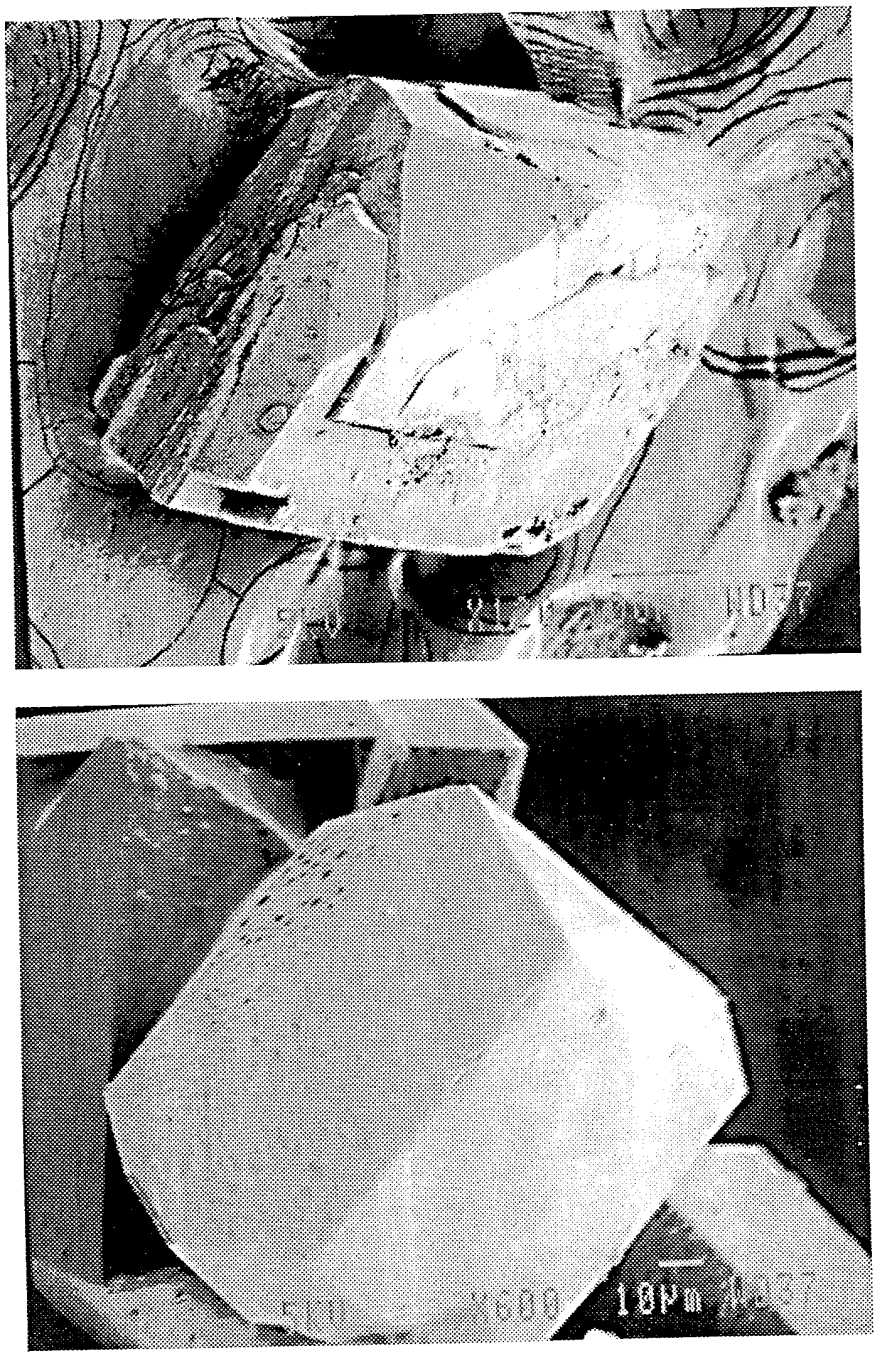

Fig. 14. CL-20 crystals grown from solution at HFMI with different particle morphologies and difect structures: (a) x120, (b) x600, (c) x40 and (d) x600.

c)

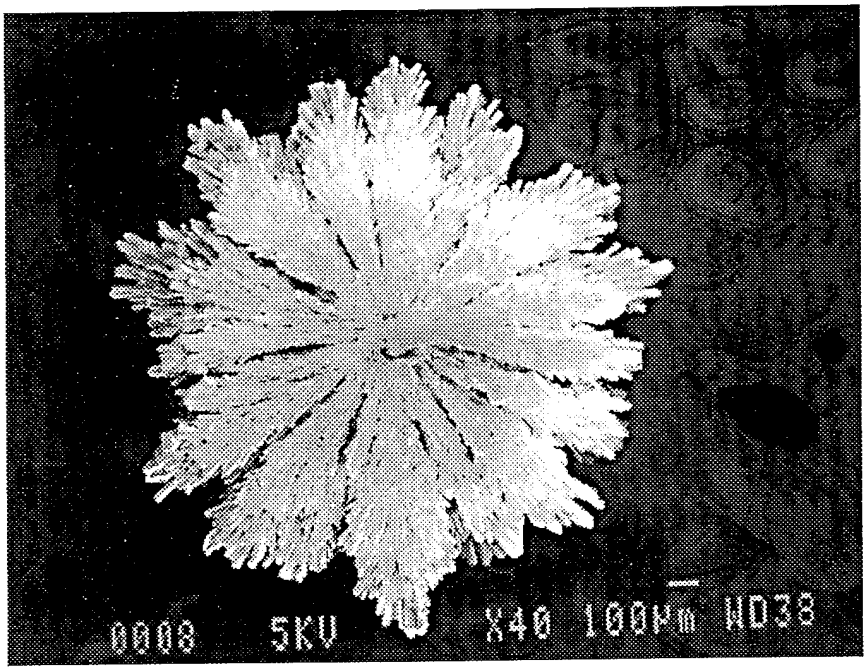

d)

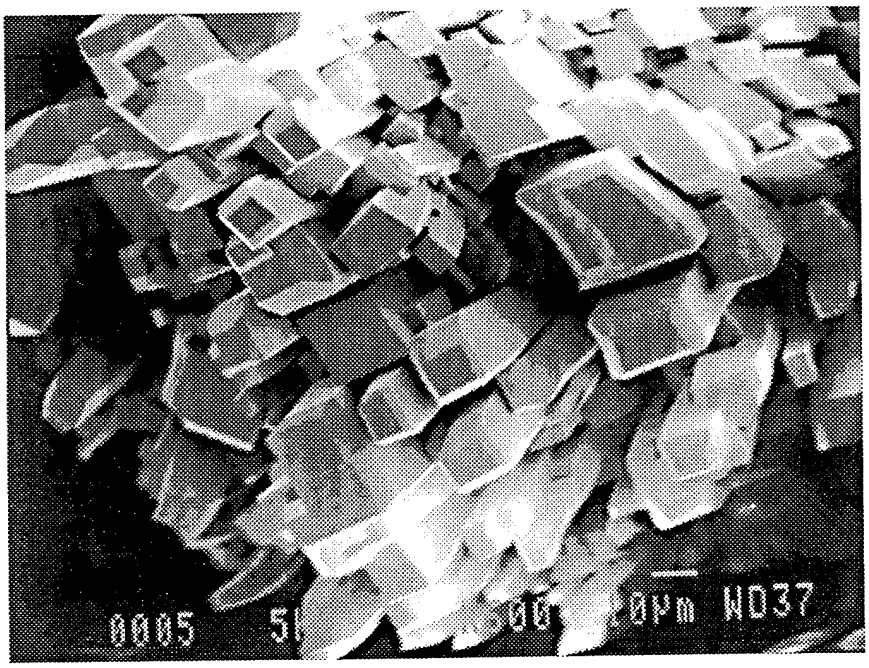

Fig. 14. CL-20 crystals grown from solution at HFMI with different particle morphologies and difect structures: (a) x120, (b) x600, (c) x40 and (d) x600.